61–94, AAAS, Washington, D.C.
Sibrack, L. A., Gray, R. H., & Bernstein, I. A. (1974) *J. Invest. Dermatol. 62*, 394–405.
Tezuka, T., & Freedberg, I. M. (1974) *J. Invest. Dermatol. 63*, 402–408.
Ugel, A. R. (1969) *Science 166*, 250–251.
Ugel, A. R. (1971) *J. Cell Biol. 49*, 405–422.
Ugel, A. R., & Idler, W. (1972) *J. Cell Biol. 52*, 453–464.
Voorhees, J. J., Chakrabarti, S. G., & Bernstein, I. A. (1968) *J. Invest. Dermatol. 51*, 344–354.

A Structural Model for Heme in High-Spin Ferric Hemoproteins. Iron Atom Centering, Porphinato Core Expansion, and Molecular Stereochemistry of High-Spin Diaquo(*meso*-tetraphenylporphinato)iron(III) Perchlorate[†]

W. Robert Scheidt,* Irwin A. Cohen, and M. E. Kastner

ABSTRACT: The synthesis and characterization of a six-coordinate high-spin ferric porphyrin, diaquo(*meso*-tetraphenylporphinato)iron(III) perchlorate ($[Fe(TPP)(OH_2)_2]ClO_4$) is described. Magnetic, Mössbauer, ESR, and structural characterization support a high-spin state ($S = {}^5/_2$) assignment. Most importantly, the structural characterization of the title compound demonstrates that the large high-spin iron(III) atom is *centered* in the heme plane, in contrast to the commonly expected out-of-plane displacement of the iron(III) atom based on the structures of a number of other high-spin ferric porphyrins. In $[Fe(TPP)(OH_2)_2]^+$, the large size of the high-spin iron(III) atom is accommodated by a radial expansion of the porphinato core with no displacement of the iron atom. The average Fe–N distance in the centrosymmetric molecule is 2.045 (8) Å, corresponding to an increase in the radius of the central hole of the porphinato ligand of ~0.055 Å relative to low-spin ferric derivatives. The axial Fe–water bond distance is 2.095 (2) Å. Crystal data for $[Fe(TPP)(OH_2)_2]ClO_4{\cdot}2THF$: $a = 16.812$ (2) Å, $b = 12.850$ (2) Å, $c = 21.346$ (2) Å, orthorhombic, space group *Pbcn*, $Z = 4$, $\rho_{calcd} = 1.38$ g/cm^3, $\rho_{obsd} = 1.39$ g/cm^3. Porphinato core expansion and concomitant centering or near centering of the iron(III) atom in the heme plane are likely to occur in a number of high-spin ferric hemoproteins, including derivatives with thermal spin equilibria. The stereochemical features of $[Fe(TPP)(OH_2)_2]^+$ provide a model for the geometry of heme in aquomethemoglobin. The data also suggest that considerable caution must be used when heme stereochemistry (coordination number) is assigned solely on magnetic properties.

The stereochemistry of porphinato complexes is of continuing interest. Especially important are studies of the stereochemistry of porphinato complexes as the metal center and axial ligands are varied systematically (Hoard, 1975; Scheidt, 1977, 1978). The structures of the iron derivatives are of immediate interest with respect to understanding the structure and function of the hemoproteins (Hoard, 1971).

For ferric porphyrins, the spin state and stereochemistry of the iron(III) center are controlled by the nature of the axial ligands. Some aspects of these phenomena are well-known. The coordination of two strong field ligands leads to low-spin six-coordinate hemes, e.g., bis(imidazole)iron(III) derivatives. Weaker field ligands, typically anionic ones such as chloride, azide, etc., lead to five-coodinate high-spin derivatives. The stereochemical features of these two classes of ferric porphyrins are also well-known, and a number of examples of each class have been structurally characterized (Hoard, 1975; Scheidt, 1978). The high-spin five-coordinate species have the iron(III) atom displaced out of the porphinato plane by ~0.5 Å with concomitant long Fe–N bonds. The low-spin six-coordinate complexes have the iron(III) atom essentially centered in the porphinato plane and relatively short Fe–N bonds. The stereochemical differences are associated with the population of the $3d_{x^2-y^2}$ orbital in the high-spin complexes and its depopulation in the low-spin complexes.

Recently we have been systematically studying ferric porphyrins coordinated to a variety of axial ligands, all of which can be described as weak field ligands. When the axial ligands are extremely weak field anionic ligands such as perchlorate (Reed et al., 1979; Dolphin et al., 1977) or tricyanomethanide [$C(CN)_3^-$] (Summerville et al., 1978), the resulting ferric porphyrin derivatives are not high spin. Rather these complexes have magnetic properties, Mössbauer spectra, and stereochemical features consistent with a ground-state assignment of intermediate spin ($S = {}^3/_2$) or a quantum mechanical admixture of $S = {}^3/_2$ and $S = {}^5/_2$ spin states (Maltempo, 1974). Both five-coordinate and six-coordinate complexes with this ground state have been structurally characterized and represent new structural types for ferric porphyrins.

The coordination of two weak field ligands to ferric porphyrins leads to still another structural type for iron(III) porphyrins, high-spin six-coordination. Ligands which lead to this type are typically neutral oxygen donor ligands (Mashiko et al., 1978): sulfoxides, dimethylformamide, pyridine *N*-oxide, triphenylphosphine oxide, and water. We report herein the preparation, characterization, and structure of one member of this class, diaquo(*meso*-tetraphenyl-

---

[†] From the Department of Chemistry, University of Notre Dame, Notre Dame, Indiana 46556 (W.R.S. and M.E.K), and the Department of Chemistry, Brooklyn College, City University of New York, Brooklyn, New York 11210 (I.A.C.). *Received March 16, 1979.* The work done at Notre Dame was supported by National Institutes of Health Grant HL-15627.

0006-2960/79/0418-3546$01.00/0

porphinato)iron(III) perchlorate, to be written as $[Fe(TPP)(OH_2)_2]ClO_4$.[1] The stereochemical features of this class provide models for the geometry of heme in high-spin hemoproteins known to have two axial ligands, viz., augomethemoglobin. Essential stereochemical features illuminated are that the high-spin iron(III) atom can lead to a substantial radial expansion of the porphinato core while remaining inplane. Thus, these results demonstrate that the high-spin state of the iron(III) atom does not require any displacement of the iron atom and further that considerable caution must be used when heme stereochemistry (coordination number) is assigned solely on magnetic properties.

Experimental Section

Synthesis and Physical Properties of $[Fe(TPP)(OH_2)]ClO_4 \cdot 2THF$. Bulk preparations of $[Fe(TPP)(OH_2)_2]^+$ were always contaminated with the oxo-bridged species $[Fe(TPP)]_2O$. Purer samples of $[Fe(TPP)(OH_2)_2]^+$ are prepared by the slow evaporation of tetrahydrofuran solutions of (perchlorato)(*meso*-tetraphenylporphinato)iron(III) (Reed et al., 1979) in the presence of perchloric acid and separation of the large single crystals produced. In a typical preparation Fe(TPP)(Cl) (1.00 g, 1.42 mmol) was dissolved in 150 mL of freshly distilled THF (CaH_2), $AgClO_4$ (0.31 g, 1.52 mmol) was added, and the solution was stirred for 4 h. The solution was filtered and 0.5 mL of 70% $HClO_4$ added. The solution was allowed to evaporate (~4 days), and large well-formed crystals were harvested. Yields ranged from 50 to 80%: IR (ν_{ClO_4}) 1140, 1115, 1085, 645, 640, 630 cm^{-1}; λ_{max} (THF) 398, 529, 615, 660 nm; ESR $g_\perp \simeq 6$, $g_\parallel \simeq 2$ (solid).

Magnetic susceptibilities were determined on a Faraday balance equipped with a Cahn-Ventron R-100 balance and a Varian Fieldial Mark I field regulated magnet. Fields of 7, 8, and 9 kG were employed at temperatures of 77, 100, 133, 165, and 298 K, and the sample was maintained in a helium atmosphere. Mössbauer data were collected as described previously (Summerville et al., 1978).

Structure Determination. A crystal with dimensions of 0.5 × 0.4 × 0.4 mm was used in all diffraction experiments. Preliminary photographic examination established a four-molecule orthorhombic unit cell. The systematic absences of $0kl$, $k \neq 2n + 1$, $h0l$, $l \neq 2n + 1$, and $hk0$, $h + k \neq 2n + 1$, lead to the uniquely probable space group $Pbcn$ ($D_{2h}{}^{14}$, No. 60). Least-squares refinement of the setting angles of 60 reflections, measured on a Syntex $P\bar{1}$ diffractometer, led to the following cell constants: (λ = 0.71073 Å) a = 16.812 (2) Å, b = 12.850 (2) Å, c = 21.346 (2) Å, and Z = 4. For a cell content of $4[FeO_2N_4C_{44}H_{32} \cdot 2C_4H_8O]$ and the above cell constants, the calculated density is 1.38 g/cm^3; the experimentally measured density is 1.39 g/cm^3.

Intensity data were measured on the automated diffractometer using graphite-monochromated Mo Kα radiation and θ–2θ scanning using experimental conditions described previously (Scheidt, 1974). Variable scan rates of 2–12°/min were employed with background counts collected at the extremes of the scan for one-half the time of the scan. A 2θ scan width of 1.9° was used, and four standard reflections were measured every 50 reflections during the course of the measurements. 3730 reflections with $F_o > 3\sigma(F_o)$ were retained as observed and used in the solution and refinement of the structure.

Table I: Atomic Coordinates in the Unit Cell of the $[Fe(TPP)(OH_2)_2]^+$ Molecule

atom type	coordinates[a] 10^4x	10^4y	10^4z
Fe	0	0	0
Cl	0	−389 (1)	1/4
N_1	218 (1)	1163 (2)	627 (1)
N_2	1172 (1)	−439 (2)	35 (1)
O_1	−255 (2)	−946 (2)	773 (1)
O_3	−154 (7)	−1387 (6)	2660 (7)
O_4	467 (6)	−402 (8)	1968 (4)
O_5	473 (4)	−39 (6)	2995 (3)
O_6	−663 (5)	240 (7)	2442 (5)
C_{a1}	−340 (2)	1823 (2)	890 (1)
C_{a2}	938 (2)	1383 (3)	909 (1)
C_{a3}	1756 (2)	33 (3)	393 (1)
C_{a4}	1536 (2)	−1179 (2)	−331 (1)
C_{b1}	52 (2)	2497 (3)	1328 (2)
C_{b2}	828 (2)	2231 (3)	1342 (2)
C_{b3}	2505 (2)	−444 (3)	242 (1)
C_{b4}	2375 (2)	−1161 (3)	−206 (1)
C_{m1}	1652 (2)	859 (2)	812 (1)
C_{m2}	−1157 (2)	1821 (2)	766 (1)
C_1	2357 (2)	1167 (3)	1191 (1)
C_2	2760 (2)	2087 (3)	1076 (2)
C_3	3415 (2)	2365 (3)	1430 (2)
C_4	3679 (2)	1732 (4)	1900 (2)
C_5	3288 (3)	818 (4)	2012 (2)
C_6	2629 (2)	536 (3)	1662 (2)
C_7	−1670 (2)	2531 (2)	1147 (1)
C_8	−2104 (2)	3329 (3)	881 (2)
C_9	−2602 (2)	3943 (3)	1243 (2)
C_{10}	−2652 (2)	3786 (3)	1879 (2)
C_{11}	−2213 (2)	3010 (3)	2150 (2)
C_{12}	−1729 (2)	2379 (3)	1792 (2)
O_2	−820 (2)	−2889 (2)	777 (1)
C_{13}	−944 (3)	−3300 (4)	1393 (2)
C_{14}	−661 (3)	−4396 (3)	1399 (2)
C_{15}	−306 (4)	−4565 (4)	773 (2)
C_{16}	−311 (3)	−3580 (4)	443 (2)
H_1	−434 (23)	−1516 (33)	756 (18)
H_2	−198 (21)	−706 (28)	1111 (17)

[a] Numbers in parentheses are the estimated standard deviations.

The structure was solved by standard heavy-atom techniques.[2] With four molecular units per cell, the $[Fe(TPP)(OH_2)_2]^+$ and ClO_4^- ions must have crystallographically required symmetry. These were found to be a required center of symmetry for $[Fe(TPP)(OH_2)_2]^+$ and a twofold axis of symmetry for the ClO_4^-. The perchlorate ion is disordered; the chlorine atom is on the twofold axis with oxygen atoms O_3, O_4, O_5, and O_6 related to atoms O_3'', O_4'', O_5'', and O_6'' by the twofold axis of symmetry. The structure was refined by full-matrix least-squares methods. A series of difference Fourier syntheses gave evidence for hydrogen atom positions of the porphinato ligand and THF solvate; these positions were idealized [C–H = 0.95 Å, B(H) = B(C) + 1.0 Å^2] and included in subsequent refinement cycles as fixed contributors. The hydrogen atoms of the unique aquo ligand were also found in a difference Fourier synthesis; their positions and isotropic temperature factors were refined in subsequent least-squares cycles. The refinement of the model was then carried to convergence by using anisotropic temperature factors for all heavy atoms and isotropic temperature factors for the hydrogens of the aquo ligand. The final values for the discrepancy indices were $R_1 = (\sum||F_o| - |F_c||)/\sum|F_o| = 0.063$ and $R_2 = [\sum w(|F_o| - |F_c|)^2/\sum w(F_o)^2]^{1/2} = 0.062$. The final data/parameter ratio was 11.7; the estimated standard deviation of an observation of unit weight was 1.56. A final

---

[1] Abbreviations used: TPP, the dianion of 5,10,15,20-tetraphenylporphyrin; THF, tetrahydrofuran; OEP, the dianion of octaethylporphyrin; TMSO, tetramethylene sulfoxide.

[2] Details of the computation can be found in Mashiko et al., 1978.

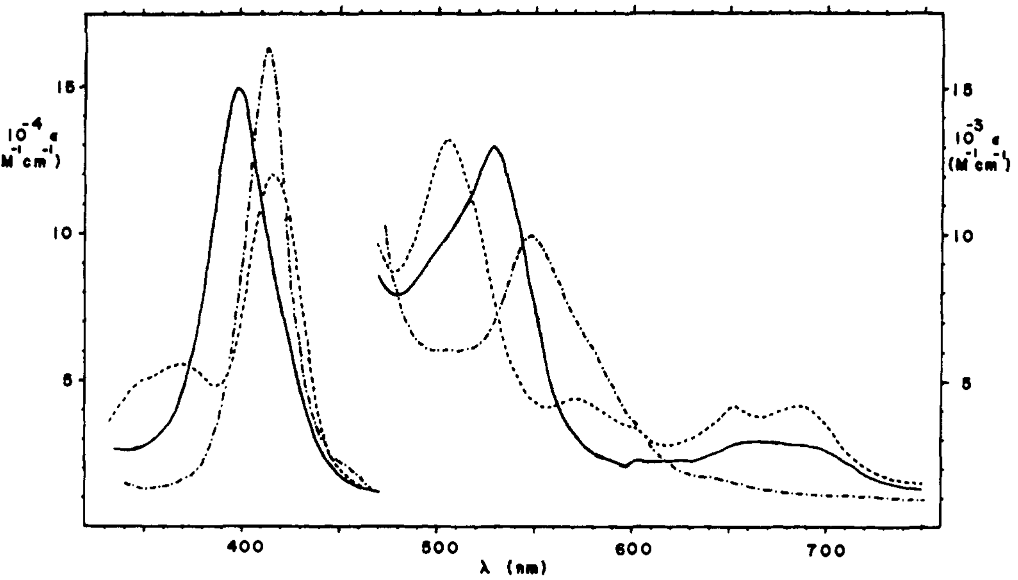

FIGURE 1: Comparison of visible spectra: $[Fe(TPP)(OH_2)_2]ClO_4$ in THF and 4% $HClO_4$ (—), Fe(TPP)(Cl) in THF (---), and $[Fe(TPP)(Im)_2]ClO_4$ in THF (-·-).

difference Fourier synthesis was judged to be essentially featureless; all peaks were less than 0.4 e/Å^3.

Final values of atomic coordinates and associated temperature factors in the asymmetric unit of structure are given in Tables I and II, respectively. A listing of the final observed and calculated structure amplitudes (×10) are available (see paragraph at end of paper regarding supplementary material).

Results and Discussion

Aquo ligands are easily introduced into the coordination sphere of an iron(III) porphyrin by displacement of coordinated perchlorate, although there are some difficulties with

$$Fe(TPP)(OClO_3) + 2H_2O \rightarrow [Fe(TPP)(OH_2)_2]ClO_4$$

preventing subsequent reaction to yield a μ-oxo derivative, $[Fe(TPP)]_2O$. $[Fe(TPP)(OH_2)_2]ClO_4$ is a six-coordinate derivative with the familiar axial ESR spectrum ($g_\perp \simeq 6$, $g_\| \simeq 2$) of high-spin ferric porphyrins. The magnetic susceptibility is substantially independent of temperature over the range 77–298 K; the effective moment, 5.6 μ_B, is slightly lower than the expected spin-only value for 5.9 μ_B for a high-spin d^5 system. A number of additional determinations at 298 K on several preparations gave μ = 5.5–5.7 μ_B. The visible spectrum of red-brown $[Fe(TPP)(OH_2)_2]^+$ is shown in Figure 1. For comparison, the spectra of high-spin Fe(TPP)(Cl) and low-spin $[Fe(TPP)(Im)_2]^+$ are also displayed in Figure 1. The Mössbauer parameters of $[Fe(TPP)(OH_2)_2]^+$ are given in Table III along with values for several other ferric heme derivatives. The Mössbauer parameters are consistent with the assignment of a high-spin state to $[Fe(TPP)(OH_2)_2]^+$. The large quadrupole splitting is indicative of the weak axial ligand field relative to the in-plane field.

Figure 2 is a computer-drawn model of the $[Fe(TPP)(OH_2)_2]ClO_4{\cdot}2THF$ molecule as it exists in the crystal. Also displayed in Figure 2 are the symbols assigned to the crystallographically unique atoms of the molecule. Bond distances in the coordination group and the aquo ligand are shown. Individual bond distances and angles are found in Tables IV and V.

Figure 2 also displays aspects of the hydrogen bonding of the aquo ligands. One proton hydrogen bonds to the oxygen atom of the THF solvate molecule with an $H_1{\cdots}O_2$ distance of 1.88 (4) Å. The other proton forms a hydrogen bond to O_4 of the perchlorate anion with an $H_2{\cdots}O_4$ distance of 2.18 Å. Perchlorate atom O_5 hydrogen bonds to an aquo proton of an adjacent $[Fe(TPP)(OH_2)_2]^+$ ion with $H_2''{\cdots}O_5$ = 2.14 (4) Å. Thus, the $[Fe(TPP)(OH_2)_2]^+$ ions are bridged by the perchlorate anions via hydrogen bonds in a chain along the *c* direction. As noted previously, the perchlorate anion is disordered; the twofold axis related orientation of the ClO_4^- group interchanges O_4 and O_5 in the hydrogen bond network. In Figure 2, only one orientation of the ClO_4^- group is shown.

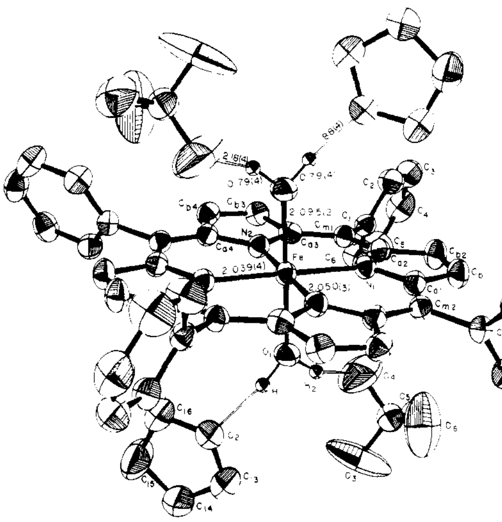

FIGURE 2: Computer-drawn model of $[Fe(TPP)(OH_2)_2]ClO_4{\cdot}2THF$. The label assigned to each crystallographically unique atom is displayed. Also shown are the unique bond distances in the coordination group. Thermal ellipsoids are contoured at the 50% probability level.

The axial $Fe{-}OH_2$ bond distance of 2.095 (2) Å is near the upper end of the observed range of $Fe{-}OH_2$ distances for high-spin ferric complexes (Hair & Beattie, 1977). Axial Fe–O distances at 2.069 (3) and 2.087 (3) Å were observed (Mashiko et al., 1978) for high-spin $[Fe(TPP)(TMSO)_2]ClO_4$. The iron to water proton distances[3] are 2.56 (4) and 2.63 (4) Å.

---

[3] These are the calculated distances based on the X-ray observed hydrogen atom positions which are known to be foreshortened. True H···Fe distances would be ~0.2 Å greater.

Table II: Thermal Parameters in $[Fe(TPP)(OH_2)_2]^+$

	anisotropic parameters^a						
atom type	B_{11}	B_{22}	B_{33}	B_{12}	B_{13}	B_{23}	B^b (Å^2)
Fe	2.57 (2)	2.41 (1)	2.15 (1)	−0.05 (2)	−0.20 (2)	−0.24 (2)	2.4
Cl	4.52 (6)	4.11 (5)	3.11 (2)	0	−0.61 (6)	0	3.8
N_1	2.7 (1)	2.4 (1)	2.3 (1)	0.0 (1)	−0.2 (1)	−0.2 (1)	2.5
N_2	2.8 (1)	2.7 (1)	2.4 (2)	−0.1 (1)	−0.2 (1)	−0.2 (1)	2.6
O_1	5.1 (1)	3.2 (1)	2.6 (1)	−1.0 (1)	0.1 (1)	−0.0 (1)	3.4
O_3	12.3 (15)	9.1 (4)	23.4 (8)	−2.0 (12)	−0.3 (13)	11.9 (10)	9.3
O_4	14.4 (8)	14.4 (8)	5.0 (4)	−2.0 (7)	3.1 (5)	−0.7 (5)	9.6
O_5	7.1 (4)	8.9 (4)	4.3 (7)	−2.1 (4)	−1.2 (3)	−0.6 (3)	6.2
O_6	9.7 (6)	11.1 (6)	14.2 (9)	6.2 (5)	−4.9 (7)	−4.7 (7)	9.2
C_{a1}	3.1 (2)	2.6 (1)	2.5 (1)	0.2 (1)	−0.0 (1)	−0.1 (1)	2.7
C_{a2}	3.0 (2)	3.0 (2)	2.4 (1)	−0.4 (1)	−0.1 (1)	−0.4 (1)	2.8
C_{a3}	2.7 (1)	2.9 (1)	2.4 (1)	−0.1 (1)	−0.4 (1)	0.3 (1)	2.6
C_{a4}	2.9 (1)	2.4 (1)	2.4 (1)	0.2 (1)	−0.0 (1)	0.1 (1)	2.6
C_{b1}	3.9 (2)	3.3 (2)	3.3 (1)	−0.2 (2)	−0.2 (1)	−1.2 (1)	3.3
C_{b2}	3.6 (2)	3.8 (2)	3.4 (1)	−0.2 (1)	−0.7 (1)	−1.3 (1)	3.4
C_{b3}	2.9 (2)	3.5 (2)	3.1 (1)	−0.1 (1)	−0.3 (1)	−0.0 (1)	3.1
C_{b4}	2.9 (2)	3.1 (2)	3.1 (1)	0.3 (2)	0.1 (1)	−0.0 (1)	3.0
C_{m1}	2.8 (1)	2.7 (1)	2.5 (1)	−0.2 (2)	−0.2 (1)	−0.2 (1)	2.7
C_{m2}	3.1 (1)	2.5 (1)	2.3 (1)	0.1 (2)	−0.1 (1)	0.0 (1)	2.6
C_1	2.7 (2)	3.3 (2)	2.3 (1)	−0.1 (1)	−0.2 (1)	−0.4 (1)	2.7
C_2	4.4 (2)	4.1 (2)	3.4 (2)	−0.6 (2)	−0.3 (2)	−0.0 (2)	3.9
C_3	4.4 (2)	5.6 (2)	5.1 (2)	−2.2 (2)	0.5 (2)	−1.6 (2)	4.5
C_4	3.6 (2)	7.6 (3)	4.4 (2)	−0.7 (2)	−1.2 (2)	−1.6 (2)	4.6
C_5	5.9 (2)	6.6 (3)	4.8 (2)	−0.6 (2)	−2.7 (2)	0.7 (2)	5.1
C_6	4.7 (2)	4.9 (2)	4.2 (2)	−1.2 (2)	−1.6 (2)	0.9 (2)	4.3
C_7	2.8 (1)	2.8 (2)	2.7 (1)	0.2 (1)	−0.2 (1)	−0.3 (1)	2.7
C_8	3.9 (2)	3.3 (2)	3.1 (2)	0.2 (1)	−0.2 (1)	0.2 (1)	3.4
C_9	4.3 (2)	2.9 (2)	5.3 (2)	1.0 (2)	−0.1 (2)	−0.3 (2)	3.9
C_{10}	3.0 (2)	5.0 (2)	4.8 (2)	0.4 (2)	0.4 (2)	−1.8 (2)	3.9
C_{11}	3.8 (2)	6.6 (2)	2.8 (2)	0.5 (2)	0.2 (2)	−0.9 (2)	4.1
C_{12}	3.4 (2)	4.1 (2)	3.3 (2)	0.8 (2)	−0.2 (1)	0.1 (2)	3.5
O_2	7.3 (2)	3.7 (1)	4.8 (1)	−0.7 (1)	1.5 (1)	−0.2 (1)	4.9
C_{13}	6.2 (2)	5.7 (3)	4.2 (2)	0.1 (2)	1.1 (2)	−0.4 (2)	5.2
C_{14}	7.3 (3)	4.7 (3)	5.7 (3)	−0.1 (2)	1.5 (2)	0.3 (2)	5.7
C_{15}	12.5 (5)	5.8 (3)	6.3 (3)	2.6 (3)	3.0 (3)	−0.3 (2)	7.1
C_{16}	8.4 (3)	5.8 (3)	5.6 (3)	−0.2 (2)	2.9 (2)	−1.1 (2)	6.0
$H_1{}^c$							6.0 (1.2)
$H_2{}^c$							4.6 (1.0)

[a] Numbers in parentheses are the estimated standard deviations. The B_{ij} values are related to the dimensionless β_{ij} values employed during refinement as $B_{ij} = 4\beta_{ij}|a_i{}^*a_j{}^*|$. [b] Isotropic thermal parameters as calculated from $B = 4[V^2 \det(\beta_{ij})]^{1/3}$. [c] Atoms refined isotropically.

Table III: Mössbauer Parameters for Selected Porphyrins

compd	spin state S	temp (K)	ΔE_Q (mm/s)	δ^a (mm/s)	ref
$[Fe(TPP)(OH_2)_2]ClO_4$	$^5/_2$	298	1.69	0.33	this work
		78	1.53	0.41	
$[Fe(TPP)(TMSO)_2]ClO_4$	$^5/_2$	4.2	1.22	0.45	Mashiko et al. (1978)
Fe(TPP)(Cl)	$^5/_2$	4.2	0.46	0.42	Maricondi et al. (1972)
Fe(TPP)(I)	$^5/_2$	78	0.70	0.69	Maricondi et al. (1972)
		6	0.75	0.72	
$[Fe(TPP)(C(CN)_3)]_n$	$^3/_2$	298	3.18	0.30	Summerville et al. (1978)
		78	3.03	0.30	
$Fe(OEP)(OClO_3)$	$^3/_2$	295	3.16	0.29	Dolphin et al. (1977)
		115	3.52	0.37	
		4.2	3.57	0.37	
$Fe(TPP)(OClO_3)$	$^3/_2$	4.2	3.4	0.39	Kastner et al. (1978)
aquomet Mb	$^5/_2$	4.2	1.3	0.4	Lang et al. (1970)
fluoromet Mb	$^5/_2$	4.2	0.8	0.4	Lang et al. (1970)
fluoromet Hb	$^5/_2$	4.2	0.7	0.4	Lang (1970)
cytochrome *c*′	$^5/_2$		1.35	0.37	Emtage et al. (1977)

[a] All values are relative to metallic Fe.

The large size of the high-spin iron(III) atom is accommodated in $[Fe(TPP)(OH_2)_2]^+$ by a substantial radial expansion of the porphinato ligand rather than an out-of-plane displacement of the iron atom typical of the five-coordinate heme derivatives (Hoard, 1975; Scheidt, 1978). The crystallographic requirement of C_i-$\bar{1}$ symmetry for the $[Fe(TPP)(OH_2)_2]^+$ ion leads to the rigorous requirement that the iron(III) atom is centered in the central hole of the porphinato ligand. The thermal parameters reported in Table II and all other features of the structural analysis are consistent with this centering of the iron(III) atom. We note that the NMR studies of Zobrist & LaMar (1978) demonstrate that this structure is maintained in solution.

Figure 3 displays the perpendicular displacements, in units of 0.01 Å, of each unique atom from the mean plane of the 24-atom core. The porphinato core is essentially planar; the

Table IV: Bond Lengths in the $[\mathrm{Fe(TPP)(OH_2)_2}]^+$ Molecule, $\mathrm{ClO_4^-}$, and the THF Solvate[a,b]

type	length (Å)	type	length (Å)	type	length (Å)
$\mathrm{Fe-N_1}$	2.039 (3)	$\mathrm{C_{a1}-C_{m2}}$	1.399 (4)	$\mathrm{C_7-C_{12}}$	1.394 (4)
$\mathrm{Fe-N_2}$	2.050 (3)	$\mathrm{C_{a4}-C_{m2}'}$	1.396 (4)	$\mathrm{O_1-H_1}$	0.793 (42)
$\mathrm{Fe-O_1}$	2.095 (2)	$\mathrm{C_{a2}-C_{m1}}$	1.392 (4)	$\mathrm{O_1-H_2}$	0.789 (36)
$\mathrm{N_1-C_{a1}}$	1.384 (4)	$\mathrm{C_{a3}-C_{m1}}$	1.398 (4)	$\mathrm{H_1-O_2}$	1.880 (43)
$\mathrm{N_1-C_{a2}}$	1.380 (4)	$\mathrm{C_1-C_2}$	1.385 (5)	$\mathrm{H_2-O_4}$	2.181 (38)
$\mathrm{N_2-C_{a3}}$	1.385 (4)	$\mathrm{C_2-C_3}$	1.382 (5)	$\mathrm{H_2-O_5''}$	2.143 (37)
$\mathrm{N_2-C_{a4}}$	1.375 (4)	$\mathrm{C_3-C_4}$	1.366 (6)	$\mathrm{Cl-O_3}$	1.352 (6)
$\mathrm{C_{a1}-C_{b1}}$	1.435 (4)	$\mathrm{C_4-C_5}$	1.368 (6)	$\mathrm{Cl-O_4}$	1.380 (8)
$\mathrm{C_{a2}-C_{b2}}$	1.441 (4)	$\mathrm{C_5-C_6}$	1.384 (5)	$\mathrm{Cl-O_5}$	1.397 (6)
$\mathrm{C_{a3}-C_{b3}}$	1.437 (4)	$\mathrm{C_6-C_1}$	1.371 (5)	$\mathrm{Cl-O_6}$	1.383 (7)
$\mathrm{C_{a4}-C_{b4}}$	1.435 (4)	$\mathrm{C_7-C_8}$	1.380 (4)	$\mathrm{O_2-C_{13}}$	1.432 (5)
$\mathrm{C_{b1}-C_{b2}}$	1.348 (5)	$\mathrm{C_8-C_9}$	1.385 (5)	$\mathrm{C_{13}-C_{14}}$	1.488 (6)
$\mathrm{C_{b3}-C_{b4}}$	1.346 (4)	$\mathrm{C_9-C_{10}}$	1.374 (5)	$\mathrm{C_{14}-C_{15}}$	1.480 (6)
$\mathrm{C_{m1}-C_1}$	1.489 (4)	$\mathrm{C_{10}-C_{11}}$	1.369 (5)	$\mathrm{C_{15}-C_{16}}$	1.449 (7)
$\mathrm{C_{m2}-C_7}$	1.496 (4)	$\mathrm{C_{11}-C_{12}}$	1.380 (5)	$\mathrm{O_2-C_{16}}$	1.424 (5)

[a] The number in parentheses following each datum is the estimated standard deviation in the last significant figure. [b] C_i and C_i' denote atoms related by the center of inversion. C_i and C_i'' denote atoms related by the twofold axis.

Table V: Bond Angles in the $[\mathrm{Fe(TPP)(OH_2)_2}]^+$ Molecule, $\mathrm{ClO_4^-}$, and the THF Solvate[a,b]

angle	value (deg)	angle	value (deg)	angle	value (deg)
$\mathrm{N_1FeN_2}$	90.3 (1)	$\mathrm{C_{m2}C_{a1}C_{b1}}$	125.2 (3)	$\mathrm{C_{13}C_{14}C_{15}}$	105.1 (4)
$\mathrm{N_1FeO_1}$	86.9 (1)	$\mathrm{C_{m1}C_{a2}C_{b2}}$	124.9 (3)	$\mathrm{C_{14}C_{15}C_{16}}$	108.0 (4)
$\mathrm{N_2FeO_1}$	90.5 (1)	$\mathrm{C_{m1}C_{a3}C_{b3}}$	125.2 (3)	$\mathrm{O_3ClO_4}$	107.8 (8)
$\mathrm{C_{a1}N_1C_{a2}}$	107.0 (2)	$\mathrm{C_{m2}C_{a4}C_{b4}}$	125.6 (3)	$\mathrm{O_3ClO_5}$	102.9 (7)
$\mathrm{C_{a3}N_2C_{a4}}$	107.5 (3)	$\mathrm{C_{a1}C_{b1}C_{b2}}$	107.8 (3)	$\mathrm{O_3ClO_6}$	115.0 (7)
$\mathrm{C_{a2}C_{m1}C_{a3}}$	124.8 (3)	$\mathrm{C_{b1}C_{b2}C_{a2}}$	107.6 (3)	$\mathrm{O_4ClO_5}$	107.5 (5)
$\mathrm{C_{a1}C_{m2}C_{a4}'}$	125.2 (3)	$\mathrm{C_{a3}C_{b3}C_{b4}}$	108.0 (3)	$\mathrm{O_4ClO_6}$	113.1 (6)
$\mathrm{N_1C_{a1}C_{m2}}$	126.0 (3)	$\mathrm{C_{b3}C_{b4}C_{a4}}$	107.6 (3)	$\mathrm{O_5ClO_6}$	109.7 (5)
$\mathrm{N_1C_{a2}C_{m1}}$	126.3 (3)	$\mathrm{C_{a2}C_{m1}C_1}$	118.5 (3)	$\mathrm{H_1O_1H_2}$	117 (4)
$\mathrm{N_2C_{a3}C_{m1}}$	126.6 (3)	$\mathrm{C_{a3}C_{m1}C_1}$	116.7 (3)	$\mathrm{O_1H_1O_2}$	175 (4)
$\mathrm{N_2C_{a4}C_{m2}}$	125.6 (3)	$\mathrm{C_{a1}C_{m2}C_7}$	117.5 (3)	$\mathrm{O_1H_2O_4}$	154 (4)
$\mathrm{N_1C_{a1}C_{b1}}$	108.8 (3)	$\mathrm{C_{a4}'C_{m2}C_7}$	117.3 (3)	$\mathrm{O_1H_2O_5''}$	161 (4)
$\mathrm{N_1C_{a2}C_{b2}}$	108.8 (3)	$\mathrm{O_2C_{13}C_{14}}$	108.1 (3)	$\mathrm{ClO_4H_2}$	114 (1)
$\mathrm{N_2C_{a3}C_{b3}}$	108.1 (3)	$\mathrm{O_2C_{16}C_{15}}$	107.7 (4)	$\mathrm{ClO_5H_2}$	115 (1)
$\mathrm{N_2C_{a4}C_{b4}}$	108.8 (3)	$\mathrm{C_{13}O_2C_{16}}$	108.6 (3)	$\mathrm{FeN_2C_{a3}}$	125.5 (2)
$\mathrm{FeN_1C_{a1}}$	126.4 (2)	$\mathrm{FeN_1C_{a2}}$	126.4 (2)	$\mathrm{FeN_2C_{a4}}$	126.7 (2)

[a] The number in parentheses following each datum is the estimated standard deviation in the last significant figure. [b] C_i and C_i' denote atoms related by the center of inversion. C_i and C_i'' denote atoms related by the twofold axis.

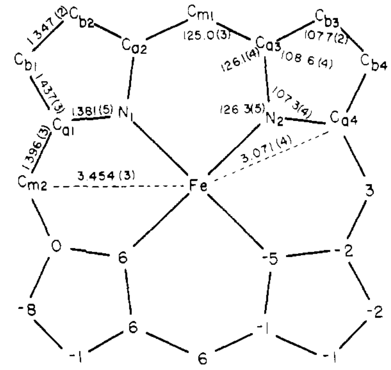

FIGURE 3: A formal diagram of the porphinato core displaying on the upper half the numbering scheme employed for the atoms of the core and average values for each type of bond length and angle. The numbers in parentheses are the estimated standard deviations. On the lower half of the centrosymmetric diagram the numbered symbol for each atom has been replaced by its perpendicular displacement, in units of 0.01 Å, from the mean plane of the porphinato core.

Table VI: Comparison of Structural Parameters in Five- and Six-Coordinate High-Spin Ferric Porphyrins

	value in	
parameter[a]	$[\mathrm{Fe(TPP)(OH_2)_2}]^+$	Fe(TPP)(I)
Fe-N	2.045	2.066
$\mathrm{C_t\cdots N}$	2.045	2.014
$\mathrm{Fe\cdots C_t}$	0.0	0.46
$\mathrm{Fe\cdots C_a}$	3.071	3.090
$\mathrm{C_t\cdots C_a}$	3.071	3.048
$\mathrm{Fe\cdots C_m}$	3.454	3.478
$\mathrm{C_t\cdots C_m}$	3.454	3.438

[a] Symbols for parameters defined in Figure 3. C_t is the symbol for the center of the porphinato ligand. All values are in angstroms.

average deviation from the mean plane is 0.034 Å. Also displayed in Figure 3 are average bond distances and angles for each chemical type in the core; these values are consistent with those expected for a radially expanded core (Hoard, 1973; Collins et al., 1972a).

The average Fe–N distance of 2.045 (8) Å is considerably longer than the 1.99-Å distance typical of low-spin ferric porphyrins (Collins et al., 1972b; Little et al., 1975; Adams et al., 1979) in which the iron(III) atom is centered in the porphinato plane. The increased Fe–N bond length is consistent with population of the $3d_{x^2-y^2}$ orbital as required for high-spin iron(III). A similar 2.045-Å value is found for the high-spin bis(tetramethylene) sulfoxide derivative of iron(III) *meso*-tetraphenylporphyrin (Mashiko et al., 1978). A Fe–N distance of 2.034 (8) Å is observed in $[\mathrm{Fe(OEP)(C_2H_5OH)_2}]\mathrm{ClO_4}$ (Einstein & Willis, 1978) in which the spin state of iron is uncertain but is probably high spin. It should be noted that these Fe–N distances, although long in comparison to low-spin values, are nonetheless ~0.02 Å shorter than the average distance observed for the high-spin, five-coordinate ferric porphyrins (Hoard, 1975; Scheidt, 1978). Table VI summarizes a number of stereochemical parameters for $[Fe(TPP)(OH_2)_2]^+$ and the corresponding value in Fe(TPP)(I), a typical five-coordinate high-spin derivative (Hatano & Scheidt, 1979).

There has been considerable recent interest in the use of X-ray absorption spectroscopy (EXAFS) to characterize the iron environment in hemoproteins (Eisenberger et al., 1976, 1978; Cramer et al., 1978). Fe–N distances are readily obtained; other important structural features such as the out-of-plane displacement of the iron atom must be calculated by triangulation on the assumption of fixed radii (particularly Ct···N). The data of Table VI, however, illustrate that the assumption of fixed radii may not be valid for ferric hemoproteins. A similar lack of fixed radii probably exists in the high-spin *iron(II)* porphyrins (Scheidt & Reed, work in progress). The data in Table VI do suggest that EXAFS measurements of the $Fe\cdots C_a$ distances as well as the Fe–N distances would give greater reliability to estimates of out-of-plane displacements.

Does radial expansion of the porphinato core occur in the prosthetic group of high-spin ferric hemoproteins? A number of observations suggest that this is the case for several derivatives. The resonance Raman spectra of aquo- and fluoromethemoglobin and myoglobin have recently been reexamined (Spiro et al., 1979) with emphasis on the three bands (II, IV, and V) shown to be sensitive to iron spin state (Spiro & Strekas, 1974; Spiro & Burke, 1976). The frequencies of these bands had been thought to be anomalously low (Spiro & Burke, 1976) and had been explained by a protein-induced doming of the porphinato core. An alternative explanation had been offered by Spaulding et al. (1975) and Warshel (1977), who suggested that the lowered frequencies were the result of porphinato core expansion. Comparison of these heme protein spectra with those obtained for high-spin bis-ligated ferric porphyrins, which our structural studies show to be planar porphyrins with expanded cores, reveals essential equivalence of the spectra. Thus, the anomalous resonance Raman spectra of these high-spin hemoproteins are adequately modelled by simple high-spin six-coordinate ferric porphyrins, and it is concluded (Spiro et al., 1979) that the hemoprotein spectra reflect core expansion. Further, the hypothesis of protein-induced doming of the core is judged untenable.

The recent refinement of the crystal structure of horse methemoglobin (Ladner et al., 1977) reveals small displacements of the iron atom from the heme plane (0.07 Å in the α chains and 0.21 Å in the β chains). Such small displacements (particularly in the α subunits), coupled with any resonable value for the Fe–N bond distance, can be consistent only with an expanded porphinato core. Weber et al. (1978) have recently suggested that porphinato core expansions are likely in erythrocruorin derivatives, although they have not yet established such an effect.

The low pH form of ferricytochrome *c* has a high-spin center (Theorell & Akesson, 1941). At least the iron–methionine bond is broken and the iron(III) atom has one (Morishima et al., 1977; Gupta & Koenig, 1971) or two (Lanir & Avirman, 1975) axial water ligands. The probable geometric correspondence between these species, especially the latter, and $[Fe(TPP)(OH_2)_2]^+$ is clear.

There has been considerable interest in hemoproteins in which the iron(III) atom has two electronic states (high and low spin) which are in thermal equilibrium with each other [for a review of methemoglobin derivatives, see Iizuka & Yonetani (1970); for rate data of the spin interconversion, see Dose et al. (1977) and Beattie & West (1974)]. Some of these hemoproteins clearly have six-coordinate iron centers. The structural data reported herein demonstrate that a possible stereochemical change for the low-spin → high-spin conversion is a simple core expansion with an *insignificant* movement of the iron atom with respect to the heme plane.

Studies of simple ferric porphyrins demonstrate that the coordination of two identical weak field ligands can lead to high-spin six-coordination with the iron atom rigorously centered in the porphinato plane. Whether the displacements of the iron atom in proteins like aquomethemoglobin are a consequence of the nonequivalent axial ligands or a feature of protein control of stereochemistry at heme (Reed, 1978; Messana et al., 1978, and references cited therein) is an interesting question. We are currently attempting to structurally characterize unconstrained synthetic porphyrin derivatives with mixed axial ligands by employing porphyrins with covalently linked ligands and by other methods.

Acknowledgments

We thank Professor P. G. Rasmussen and L. Garber for access to magnetic balances and Professor T. G. Spiro for a preprint of his resonance Raman experiments. We also thank Professor R. G. Hayes for ESR measurements.

Supplementary Material Available

A table of observed and calculated structure factors (×10) (17 pages). Ordering information is given on any current masthead page.

References

Adams, K. M., Rasmussen, P. G., Scheidt, W. R., & Hatano, K. (1979) *Inorg. Chem.* (in press).

Beattie, J. K., & West, R. J. (1974) *J. Am. Chem. Soc. 96*, 1933.

Collins, D. M., Scheidt, W. R., & Hoard, J. L. (1972a) *J. Am. Chem. Soc. 94*, 6689.

Collins, D. M., Countryman, R., & Hoard, J. L. (1972b) *J. Am. Chem. Soc. 94*, 2066.

Cramer, S. P., Dawson, J. H., Hodgson, K. O., & Hager, L. P. (1978) *J. Am. Chem. Soc. 100*, 7282.

Dolphin, D. H., Sams, J. R., & Tsin, T. B. (1977) *Inorg. Chem. 16*, 711.

Dose, E. V., Tweedle, M. F., Wilson, L. J., & Sutin, N. (1977) *J. Am. Chem. Soc. 99*, 3886.

Einstein, F. W. B., & Willis, A. C. (1978) *Inorg. Chem. 17*, 3040.

Eisenberger, P. N., Shulman, R. G., Brown, G. S., & Ogawa, S. (1976) *Proc. Natl. Acad. Sci. U.S.A. 73*, 491.

Eisenberger, P. N., Shulman, R. G., Kincaid, B. M., Brown, G. S., & Ogawa, S. (1978) *Nature* (*London*) *274*, 30.

Emtage, M. T., Zimmerman, R., Que, L., Munck, E., Hamilton, W. D., & Orme-Johnson, W. H. (1977) *Biochim. Biophys. Acta 495*, 12.

Gupta, R. K., & Koenig, S. H. (1971) *Biochem. Biophys. Res. Commun. 45*, 1134.

Hair, N. J., & Beattie, J. K. (1977) *Inorg. Chem. 16*, 245.

Hatano, K., & Scheidt, W. R. (1979) *Inorg. Chem. 18*, 877.

Hoard, J. L. (1971) *Science 174*, 1295.

Hoard, J. L. (1973) *Ann. N.Y. Acad. Sci. 206*, 18.

Hoard, J. L. (1975) in *Porphyrins and Metalloporphyrins* (Smith, K. M., Ed.) pp 317–380, Elsevier, Amsterdam.

Iizuka, T., & Yonetani, T. (1970) *Adv. Biophys. 1*, 157.

Kastner, M. E., Scheidt, W. R., Mashiko, T., & Reed, C. A. (1978) *J. Am. Chem. Soc. 100*, 666.

Ladner, R. C., Heidner, E. J., & Perutz, M. F. (1977) *J. Mol. Biol. 114*, 385.

Lang, G. (1970) *Q. Rev. Biophys. 3*, 1.

Lang, G., Asakura, T., & Yonetani, T. (1970) *Biochim. Biophys. Acta 214*, 381.

Lanir, A., & Aviram, I. (1975) *Arch. Biochem. Biophys. 166*, 439.

Little, R. G., Dymock, K. R., & Ibers, J. A. (1975) *J. Am. Chem. Soc. 97*, 4532.

Maltempo, M. M. (1974) *J. Chem. Phys. 61*, 2540.

Maricondi, C., Straub, D. K., & Epstein, L. M. (1972) *J. Am. Chem. Soc. 94*, 4157.

Mashiko, T., Kastner, M. E., Spartalian, K., Scheidt, W. R., & Reed, C. A. (1978) *J. Am. Chem. Soc. 100*, 6354.

Messana, C., Massimo, C., Shenkin, P., Noble, R. W., Fermi, G., Perutz, R. N., & Perutz, M. F. (1978) *Biochemistry 17*, 3652.

Morishima, I., Ogawa, S., Yonezawa, T., & Iizuka, T. (1977) *Biochim. Biophys. Acta 495*, 287.

Reed, C. A. (1978) in *Metal Ions in Biological Systems* (Sigel, H., Ed.) Vol. 7, Chapter 7, Marcel Dekker, New York.

Reed, C. A., Mashiko, T., Bentley, S. P., Kastner, M. E., Scheidt, W. R., Spartalian, K., & Lang, G. (1979) *J. Am. Chem. Soc. 101*, 2948.

Scheidt, W. R. (1974) *J. Am. Chem. Soc. 96*, 84.

Scheidt, W. R. (1977) *Acc. Chem. Res. 10*, 339.

Scheidt, W. R. (1978) in *The Porphyrins* (Dolphin, D. H., Ed.) Vol. III, pp 463–511, Academic Press, New York.

Spaulding, L. D., Chang, C. C., Yu, N. T., & Felton, R. H. (1975) *J. Am. Chem. Soc. 97*, 2517.

Spiro, T. G., & Strekas, T. C. (1974) *J. Am. Chem. Soc. 96*, 338.

Spiro, T. G., & Burke, J. M. (1976) *J. Am. Chem. Soc. 98*, 5482.

Spiro, T. G., Strong, J. D., & Stein, P. (1979) *J. Am. Chem. Soc. 101*, 2648.

Summerville, D. A., Cohen, I. A., Hatano, K., & Scheidt, W. R. (1978) *Inorg. Chem. 17*, 2906.

Theorell, H., & Akesson, A. (1941) *J. Am. Chem. Soc. 63*, 1812.

Warshel, A. (1977) *Annu. Rev. Biophys. Bioeng. 6*, 273.

Weber, E., Steigemann, W., Jones, T. A., & Huber, R. (1978) *J. Mol. Biol. 120*, 327.

Zobrist, M., & LaMar, G. N. (1978) *J. Am. Chem. Soc. 100*, 1944.

Investigation of the Interactions of Oxytocin with Neurophysins at Low pH Using Carbon-13 Nuclear Magnetic Resonance and Carbon-13-Labeled Hormones[†]

Michael Blumenstein,* Victor J. Hruby,* and V. Viswanatha

ABSTRACT: The specifically ^{13}C-labeled (90% ^{13}C-enriched) peptide hormone derivatives [1-hemi[2-^{13}C]cystine]oxytocin, [1-hemi[1-^{13}C]cystine]oxytocin, and [2-[2-^{13}C]tyrosine]-oxytocin and the analogue [3-[2-^{13}C]leucine]oxytocin were prepared by total synthesis and used to study the interactions of the neurohypophyseal hormones with the bovine neurophysins as a function of pH and temperature. Under all conditions, whether high or low pH, the chemical shifts of the labeled carbon atoms of the bound hormones are the same, but they are shifted significantly from their positions in the free hormone. These results indicate that interactions of the side chain and disulfide moieties of the hormone with the neurophysins do not change as a function of pH. At neutral pH and 20–35 °C, the labeled atoms of the hormone are in slow exchange (1–5 s^{-1}) with the neurophysins for the above hormone derivatives, but at low pH they are in intermediate or fast exchange depending upon the pH and temperature. At low pH, the dissociation rate constant (k_{off}) is about 100-fold greater than the value at neutral pH, and this increase appears to be due exclusively to the breaking of the salt bridge involving the N-terminal amino group of oxytocin and a side-chain carboxyl group of neurophysin. Since the dissociation constant (K_{d}) also increases by about 100-fold in going from neutral to low pH, the association rate constant is deduced to be the same at neutral and low pH. In contrast to the low pH results, an increase in pH (from 6.6 to 10.5) leads to a continual decrease in the binding constant but to no apparent change in the dissociation rate constant. The bound hormone is always in slow exchange at high pH, even when the binding constant has been reduced by 2 or 3 orders of magnitude. At high pH, the decrease in binding affinity is due solely to the deprotonation of the α-amino group of the free hormone. Thus, at high pH the apparent association rate constant decreases, while the dissociation rate constant remains unchanged.

The interaction of the neurohypophyseal hormone oxytocin with a group of proteins known as neurophysins provides a unique system for investigating peptide hormone–macromolecular interactions, and a large number of studies on this system have been carried out (for reviews, see Breslow, 1974; Walter, 1975). Most of these studies have been conducted at a pH which was close to neutrality though some studies at other pH values have been done. By measuring binding constants as function of pH, it has been found that two groups, one with a pK_{a} of about 6.5 and the other with a pK_{a} of 4.5, are important for binding (Camier et al., 1973). From studies with oxytocin analogues, it was deduced that the group with a pK_{a} of 6.5 probably is the N-terminal group of free oxytocin

---

[†] From the Departments of Chemistry and Biochemistry, University of Arizona, Tucson, Arizona 85721 (V.J.H. and V.V.), and the Department of Biochemistry and Pharmacology, Tufts University, School of Medicine, Boston, Massachusetts, 02111 (M.B.). *Received January 25, 1979.* This research was supported by grants from the U.S. Public Health Service, HD-10616 (M.B.) and AM-17420 (V.J.H.). Experiments on the Bruker HX-270 were performed at the Francis Bitter National Magnet Laboratory of the Massachusetts Institute of Technology which is supported by National Science Foundation Contract C-670 and National Institutes of Health Grant RR-00995.

0006-2960/79/0418-3552$01.00/0